Multifractal phenomena in physics and chemistry

H. Eugene Stanley* & Paul Meakin†

* Center for Polymer Studies and Department of Physics, Boston University, Boston, Massachusetts 02215, USA
† Central Research and Development Department, E. I. du Pont de Nemours and Company, Experimental Station, Wilmington, Delaware 19898, USA

The neologism 'multifractal phenomena' describes the concept that different regions of an object have different fractal properties. Multifractal scaling provides a quantitative description of a broad range of heterogeneous phenomena.

A WIDE range of complex structures of interest to physicists and chemists have in recent years been quantitatively characterized using the idea of a fractal dimension; a dimension that corresponds in a unique fashion to the geometrical shape under study and that often is not an integer[1-7]. The key to this progress has been the recognition that many objects with random structure possess a scale symmetry. Scale symmetry implies that objects look the same on many different scales of observation.

To be more specific, consider an object with fractal dimension d_f. Imagine that we digitize the object by representing it by the pixels of a computer. If a unit mass is associated with each pixel, the total mass M of the object corresponds to its volume and its 'density' $\rho \equiv M/L^d$ is a measure of the fraction of d-dimensional space occupied by the object. Here L is a characteristic diameter, such as the caliper diameter or radius of gyration. If, however, $d_f < d$, the mass increases more slowly than L^d as the size of the object increases; for example, if we double L ($L \rightarrow L' = 2L$) then M increases by a power less than 2^d (that is, $M \rightarrow M' = 2^{d_f}M < 2^d M$). Thus the density decreases ($\rho \rightarrow \rho' = 2^{d_f - d}\rho < \rho$).

As long as a unit mass is associated with each pixel, a single scaling exponent d_f characterizes the structure of the object. In recent years, however, very interesting phenomena have been studied which seem to require not one but an infinite number of exponents for their description. Such multifractal phenomena have recently become an extremely active area of investigation and here we provide the non-specialist with a brief introduction to them. There are many types of multifractal phenomena but we shall concentrate on two examples, the behaviour of complex surfaces and interfaces[8], and fluid flow in porous media.

Complex surfaces

Figure 1a shows an object formed by a process called diffusion-limited aggregation (DLA)[9,10]; such structures arise naturally in many processes currently of interest to physicists and chemists, ranging from electrochemical deposition[11,12], thin-film

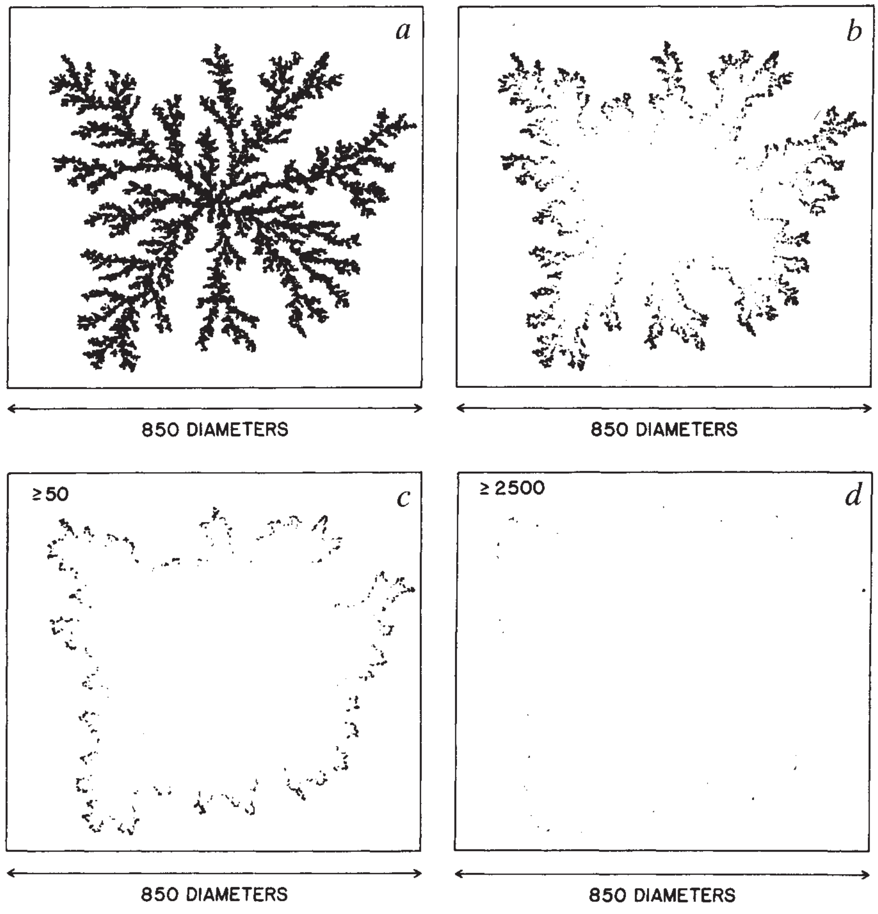

Fig. 1 The harmonic measure for a 50,000 particle off-lattice two-dimensional DLA aggregate. a, The cluster; b, all 6,803 perimeter sites that have been contacted by at least one out of 10^6 random walkers, following off-lattice trajectories. c, All the perimeter sites that have been contacted 50 or more times. d, The sites that have been contacted 2,500 or more times. The maximum number of contacts for any perimeter site 8,197, so that $p_{max} = 8.2 \times 10^{-3}$ (after ref. 27).

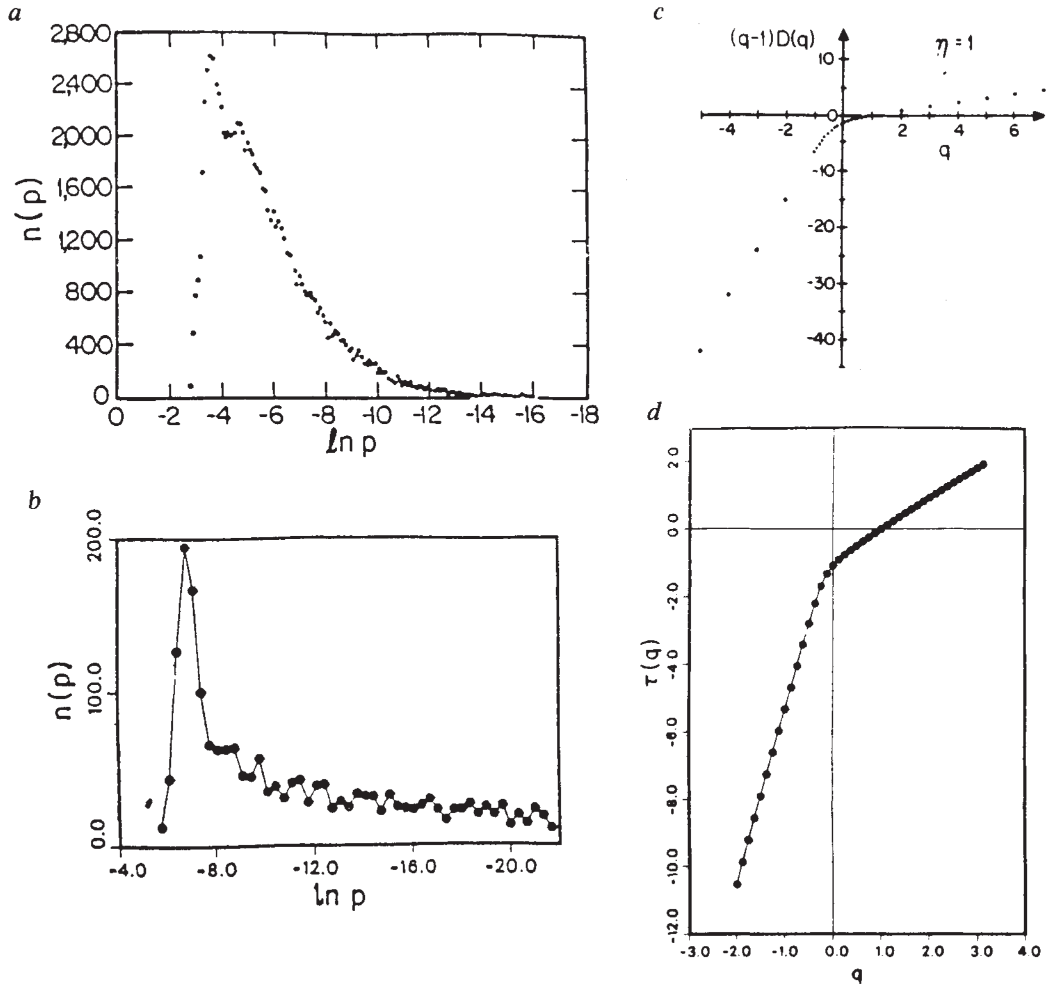

Fig. 2 Comparison between: *a*, *b*, the distribution functions $n(p)$ and *c*, *d*, the critical exponents $\tau(q)=(q-1)D(q)$ for viscous fingering patterns. *a*, Theoretical and experimental values for $n(p)$, where $n(p)\delta p$ is the number of perimeter sites with growth probabilities in the range $[p, p+\delta p]$. The simulated patterns and their growth probabilities were obtained[31] using the dielectric breakdown model. The growth probabilities for the experimental patterns were obtained by numerically solving Laplace's equation in the vicinity of a digitized representation of the pattern with absorbing boundary conditions on the sites occupied by the pattern. Similar results were obtained for small α by directly subtracting two successive experimental patterns. *c*, Theoretical and (*d*) experimental values for $\tau(q)$ in both cases was obtained numerically as in *a* and *b* (refs 31 and 32).

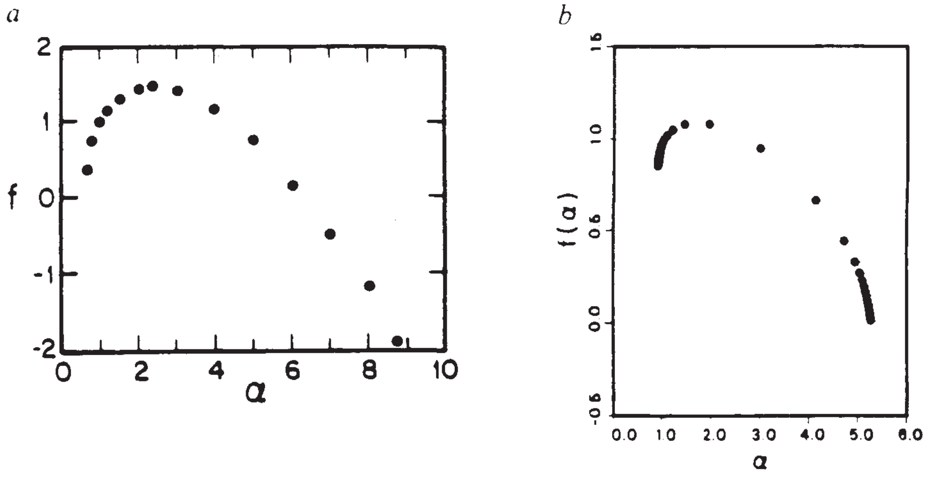

Fig. 3 Comparison between theoretical (*a*) and experimental (*b*) plots of the function $f(\alpha)$ (see Box 1) (refs 31 and 32).

morphology[13] and dendritic solidification[14-17] to various 'breakdown phenomena' such as dielectric breakdown[18,19] viscous fingering[20-24], and chemical dissolution[25,26]. If patterns such as the one shown in Fig. 1*a* are digitized, the fractal dimension $d_f \approx 1.7$ is obtained. Thus $d_f - d = -0.3$, and ρ decreases as the object grows due to the presence of 'fjords' whose size increases as the DLA cluster grows.

What is meant by the surface of the DLA cluster in Fig. 1*a* depends on the way it is to be measured. The exposed tips define one surface that is most likely to matter when diffusion is the essential feature, for example, if the surface is probed by particles undergoing random-walk motion. Figure 1*b*–*d* shows where the same object has been 'hit' by 10^6 random walkers[27], highlighting the surface sites touched by one, 50 and 2,500 random walkers respectively. Any of these three figures could be used to define the accessible surface, but the actual surfaces shown in Fig. 1*b*–*d* differ a great deal from one another. This example emphasizes that there is no unambiguous definition of the surface of this object.

An unambiguous quantity is the 'hit probability' p_i, defined as the probability that surface site i is the next to be hit. Operationally, we calculate $p_i \equiv N_i/N_T$, where N_i is the number

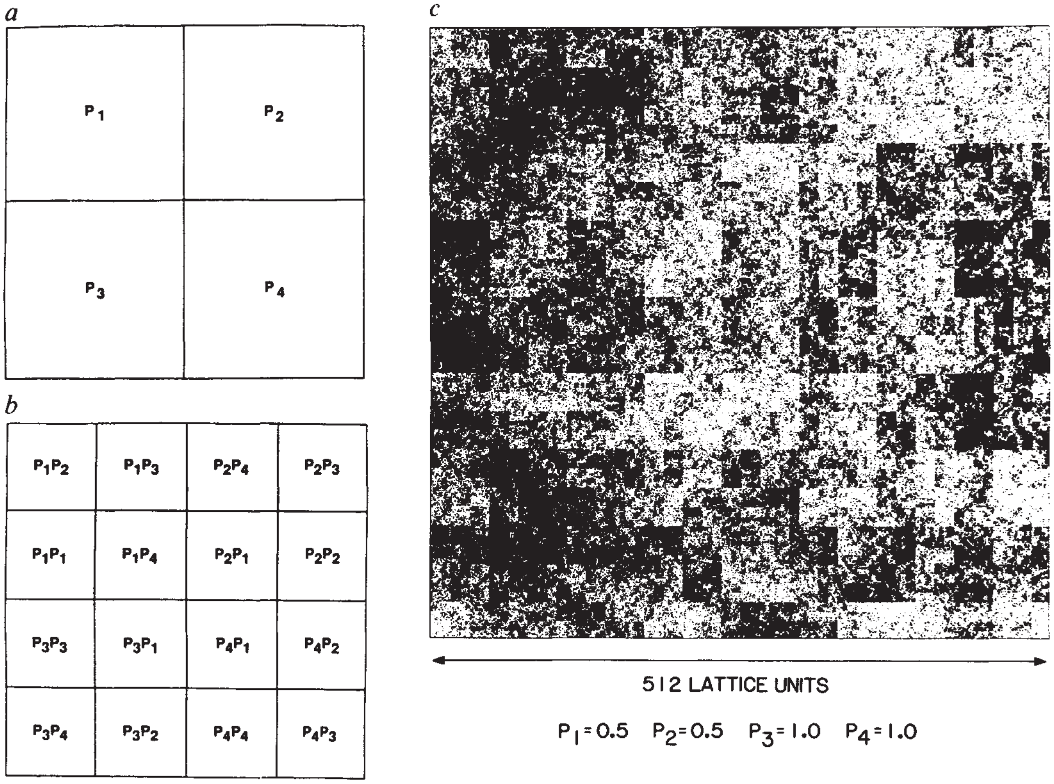

Fig. 4 A multifractal lattice: *a*, generator; *b*, second stage of construction; *c*, results after 8 generations. Lattice shown contains 2^8 pixels along each edge and shading is proportional to the value of π_i for pixel *i*. Here π_i is the product of the 8 probabilities assigned to that pixel as a result of the 8 generations (ref. 61).

of trajectories that hit site *i* and $N_T \equiv \sum_i N_i$ is the total number of trajectories (for the example of Fig. 1 $N_T = 10^6$). The set of numbers p_i may be used to form a probability distribution function $n(p)$, where $n(p)\delta p$ is the number of p_i in the range $[p, p+\delta p]$, as shown in Fig. 2. This probability distribution, like all probability distributions, is characterized by its moments

$$Z(q) \equiv \sum_p n(p)p^q \qquad (1)$$

A central dogma of critical point phenomena has been the statement that the probability distributions that arise are characterized by only two independent exponents[28]. This means that we obtain no more information about the system by studying increasingly higher moments: moment $q+1$ is described by an exponent related to that of moment q by a simple gap exponent Δ. In general, one finds that

$$Z(q) \sim L^{-\tau(q)} \qquad (2)$$

If the central dogma were correct, then $\tau(q)$ would be a linear function of q so that only *two* independent exponents would be needed to specify $\tau(q)$. It was discovered recently that this idea fails for the probability distribution $n(p)$ for DLA: both simulation[27,29–31], (Fig. 2*c*) and experiments[32] (Fig. 2*d*) show that $\tau(q)$ is a continuous curve. An infinite hierarchy of independent exponents is required. The Legendre transform $f(\alpha)$ of the function $\tau(q)$ contains the same information as $\tau(q)$ itself (see Fig. 3 and Box A), and is the characteristic customarily studied when dealing with multifractals[27,30–42].

Fluid flow in complex media

Consider a second example, fluid flow in random porous media. Such flow is customarily represented by considering an idealized network of bonds, a fraction p of which are open, and the remaining fraction $1-p$ of which are blocked[43]. For p lower than a critical value p_c, termed the percolation threshold, no fluid passes across a macroscopic system. At p_c a single macroscopic cluster appears, called the incipient infinite cluster, which carries fluid across the entire system. The singly connected bonds

A. Analogies of multifractals with thermodynamics and multifractal scaling

Consider the sum in equation (1) in the form

$$Z(q) = \sum_p e^{F(p)} \qquad (A1)$$

where

$$F(p) = \log n(p) + q \log p \qquad (A2)$$

The sum in (A1) is dominated by some value $p = p^*$, where p^* is the value of p that maximizes $F(p)$. Thus

$$Z(q) \sim e^{F(p^*)} = n(p^*)(p^*)^q \qquad (A3)$$

For fixed q, p^* and $(n(p^*)$ both depend on the system size L, leading one to define the new q-dependent exponents α and f by

$$p^* \sim L^{-\alpha}; \qquad n(p^*) \sim L^f \qquad (A4)$$

Substituting (A4) into (A3) gives

$$Z(q) \sim L^{f-\alpha q} \qquad (A5)$$

Comparing (A5) with equation (2), we find the desired result

$$\tau(q) = q\alpha(q) - f(q). \qquad (A6)$$

From (A2) it follows that

$$\frac{d}{dq}\tau(q) = \alpha(q). \qquad (A7)$$

Hence we can interpret $f(\alpha)$ as the negative of the Legendre transform of the function $\tau(q)$

$$f(\alpha) = -(\tau(q) - q\alpha) \qquad (A8)$$

where $\alpha \equiv d\tau/dq$. The function $Z(q)$ is formally analogous to the partition function $Z(\beta)$ in thermodynamics, so that $\tau(\beta)$ is like the free energy. The Legendre transform $f(\alpha)$ is thus the analogue of the entropy, with α being the analogue of the energy *E*. Indeed, the characteristic shape of plots of $f(\alpha)$ against α (compare Fig. 3) are reminiscent of plots of the dependence on *E* of the entropy for a thermodynamic system.

B. Random multiplicative processes
[A cautionary note for random sampling algorithms]

Multifractal phenomena seem to be associated with systems where the underlying physics is governed by a random multiplicative process. A simple random additive process might be the sum of 8 numbers, each number being chosen to be either $a-1$ or $a+1$ (this has a geometrical interpretation as an 8-step random walk on a one-dimensional lattice). Similarly, a simple random multiplicative process could be the product of 8 numbers, each number randomly chosen to be either a $1/2$ or $a/2$ (S. Redner, personal communication). The results of simulations of such a process are shown in Fig. 5. The y-axis is the running average of the product after R realizations and the x-axis is the number of realizations R.

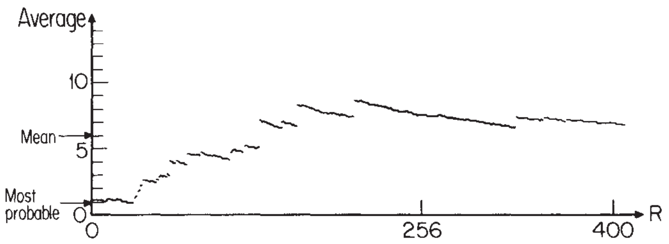

Fig. 5 A computer simulation of a random multiplicative process in which a string of 8 numbers is multiplied together. Each number is chosen with equal probability to be either 2 or 1/2. The limiting or asymptotic value of the product is $(5/4)^8 = 5.96$. The simulations do not give this value unless the number of realizations R is approximately the same as the total number of configurations of this product, $2^8 = 256$. Simulation provided by R. Selinger.

In total there are 2^8, or 256, possible configurations of such random products. Normally, random sampling procedures give approximately correct answers when only a small fraction of the possible 256 configurations has been realized. Here, however, one sees from Fig. 5 that the correct asymptotic value of the product is attained only after ~256 realizations (S. Redner, personal communication). Monte Carlo sampling of only a small fraction of the 256 configurations is doomed to failure because a rare few configurations—consisting, of, say, all 2s or seven 2s and a single 1—bias the average significantly and give rise to the upward steps in the running average shown in Fig. 5.

A simple random multiplicative process that gives rise to multifractal phenomena is found in the simple hierarchical model of the percolation backbone shown in Fig. 6. If the potential drop across the singly connected links is V_1 and that across the multiply-connected links is V_2, then when this structure is iterated, the potential drops across each of the bonds are products of the potential drops of the original structure. For this hierarchical structure $Z(q) = (V_1^q + V_2^q)^N$, where N is the number of iterations carried out. It turns out that $Z(q)$ obeys a power-law relation of the form of equation (2), with an infinite hierarchy of exponents given by $\tau(q) = 1 + \log[V_1^q + V_2^q]/\log 2$. To obtain this result, the relation $N_1 = L^{3/4}$ must be used, where N_1 is the number of singly connected bonds[54–57].

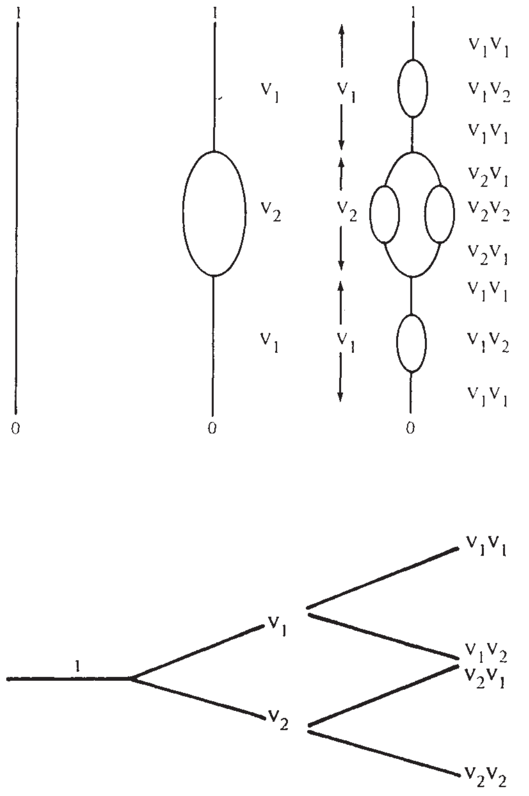

Fig. 6 A hierarchical model of the percolation backbone which displays multifractal scaling of the potential distribution $n(V)$. A unit potential is applied across the extremities of the cluster. The potentials shown are given by $V_1 = 2/5$ and $V_2 = 1/5$ (after ref. 37).

of this incipient infinite cluster carry the entire current and so sustain the largest potential drops, whereas the multiply connected bonds partition the current among them and so have smaller potential drops. The analogue of the hit-probability distribution $n(p)$ for DLA is the potential-drop distribution $n(V)$, where $n(V)\,dV$ is the number of bonds whose current lies in the interval $[V, V+dV]$[44–53]. The distribution $n(V)$ is characterized by its moments and the analogue of (1) is $Z(q) = \sum n(V) V^q$. If the size of the random network is doubled, the distribution function $n(V)$ changes and so do the moments $Z(q)$. An infinite hierarchy of exponents $\tau(q)$ is found and again $\tau(q)$ is not linear in q.

It is natural to ask why the constant gap or single exponent idea breaks down when studying the surface of a DLA cluster. The key idea is that the underlying probability distribution $n(p)$ develops a long 'tail' extending to extremely small values of the variable p (Fig. 2). For DLA, this tail arises from the presence of extremely deep cluster 'fjords'. As the cluster grows, the hit probability p_i for all cluster sites decreases. The hit probability p_i for a site deep in a fjord, however, decreases much faster than p_i for a site on the exposed tips. Thus the long tail of the $n(p)$ distribution shifts its relative weight to smaller and smaller values of p as the cluster grows.

Similarly for flow in porous media, the distribution function $n(V)$ has a long tail extending to extremely small values of the potential V. This tail arises from the presence of large multiply connected regions of the network, termed blobs[54–57]. When $L \to L' = 2L$, the characteristic size of the largest blobs increases from M to $M' = 2^{1.62}M$ (ref. 58). Thus the minimum potential drops decrease dramatically and the distribution function $n(V)$ has a larger fraction of its weight from very small values of V.

Generality

It is not necessary to have a fractal structure to find multifractal phenomena. For example, consider the electric field E_i at every point i on the surface of a charged needle—a non-fractal object of dimension one. The set $\{E_i\}$ of electric-field values is formally analogous to the set $\{p_i\}$ of DLA growth probabilities, and indeed one finds that the $\{E_i\}$ also form a multifractal set[27,35]. A question that arises naturally concerns the conditions under which multifractal phenomena can be expected. As the example of the needle suggests, it is necessary to define a 'measure' on an object such that this measure has a different fractal dimension in different regions of the object[59]. Thus when the length of a needle is doubled, the electric field near its tip changes by a factor which differs from the factor by which the electric field near the centre changes. Similarly, when the mass of DLA is doubled, the growth probability near the tips of a DLA structure changes by a factor different from the growth probability deep in the fjords. This is because the screening in the deep fjords increases dramatically with increasing cluster size.

Multifractal theory permits the characterization of complex phenomena in a fully quantitative fashion. Just as completely random phenomena in nature may generate shapes that are fractal, phenomena with spatial correlations are sometimes multifractals. For example, randomly porous media are traditionally modelled by the random-resistor network of percolation theory: the resistance of each element corresponds to the permeability in a suitable digitization of the porous medium Although this model captures much of the essential physics, it neglects the phenomenon of spatial correlation that in turn leads to both short- and long-range heterogeneities in the porous medium. For this reason, it has been recently proposed that atmospheric turbulence and porous media should be modelled by a multifractal lattice[60-64]. This is obtained by a random multiplicative process (see Fig. 4 and Box B). Transport in such a lattice can be anomalously slow, just as it is in the random-resistor network model. But the exponent d_w describing the anomaly can be continuously tuned; in fact the slowing down can, under suitable conditions, become large without limit. A similar model has been solved analytically in one dimension[76].

Analogous phenomena are found for a wide variety of systems; in fact, multifractal phenomena were first found in studies of fluid turbulence[65,66], and in analysis of non-linear dynamical systems[67-69]. Recently it has been demonstrated[33] that experimental data concerning the onset of turbulence can be analysed using a method derived from multifractal theory. Various multifractal sets have been mapped on to the thermodynamics of one-dimensional spin models[70]. In a study of the depletion of a diffusion substance near an absorbing polymer it has been found that the scaling with distance r of each moment of the Laplace field is governed by an independent exponent[71].

Several authors have examined the multifractal properties of random walks[72-74]. In particular, it has been shown[72-74] that the fractal dimension d_f is a member of a continuous set of scaling exponents; consideration of the entire hierarchy of scaling exponents provides a more complete description of random walks than was possible previously. The main idea is to characterize an infinite walk with an exponent α that measures how fast its total probability decays to zero with increasing mass of the walk. The analogue of the function $f(\alpha)$ discussed above is the growth rate $z(\alpha)$ for the subset of walks with decay rate α. The analogue of $\tau(q)$ is the Legendre transform of $z(\alpha)$. A log-normal distribution has been found for the first-passage time in percolation[77], and some understanding of the conditions under which such a log-normal distribution will occur has also developed recently[37,75].

We thank our collaborators P. Alstrøm, A. Coniglio, G. Daccord, T. C. Halsey, J. Nittmann, I. Procaccia, D. Stassinopoulos, E. Touboul and T. A. Witten. We are also grateful to C. Amitrano, L. de Arcangelis, F. di Liberto, L. Pietronero and S. Redner for helpful discussions. A. Bunde, P. Grassberger and S. Havlin commented on the first draft of this article. The work at Boston University was supported by grants from NSF and ONR.

1. Mandelbrot, B. B. *The Fractal Geometry of Nature* (Freeman, San Francisco, 1982).
2. Family, F. & Landau, D. P. (eds) *Kinetics of Aggregation and Gelation* (Elsevier, Amsterdam, 1984).
3. Stanley, H. E. & Ostrowsky, N. (eds) *On Growth and Form: Fractal and Non-Fractal Patterns in Physics* (Nijhoff, Dordrecht, 1985).
4. Boccara, N. & Daoud, M. (eds) *Physics of Finely Divided Matter* (Springer, Heidelberg, 1985).
5. Pynn, R. & Skjeltorp, A. (eds) *Scaling Phenomena in Disordered Systems* (Plenum, New York, 1986).
6. Pietronero, L. & Tosatti, E. (eds) *Fractals in Physics* (North-Holland, Amsterdam, 1986).
7. Stanley, H. E. *Introduction to Fractal Phenomena* (Oxford University Press, in the press).
8. Meakin, P. *CRC Critical Rev. in Solid State and Materials Sciences* **13**, 143-189 (1987).
9. Witten, T. A. & Sander, L. M. *Phys. Rev. Lett.* **47**, 1400-1403 (1981); *Phys. Rev.* B **27**, 5686-5697 (1983).
10. Sander, L. M. *Nature* **332**, 789-793 (1986); *Scient. Am.* **256**, 94-100 (1986).
11. Brady, R. M. & Ball, R. C. *Nature* **309**, 225-229 (1984).
12. Matsushita, M., Sano, M., Hakayawa, Y., Honjo, H. & Sawada, Y. *Phys. Rev. Lett.* **53**, 286-289 (1984).
13. Elam, W. T. *et al. Phys. Rev. Lett.* **54**, 701 (1985).
14. Ben-Jacob, E. *et al. Phys. Rev. Lett.* **55**, 1315-1318 (1985).
15. Buka, A., Kertèsz, J. & Vicsek, T. *Nature* **323**, 424-425 (1986).
16. Couder, Y., Cardoso, O., Dupuy, D., Tavernier, P. & Thom, W. *Europhys. Lett.* **2**, 437-443 (1986).
17. Nittmann, J. N. & Stanley, H. E. *Nature* **321**, 663-668 (1986).
18. Niemeyer, L., Pietronero, L. & Wiesmann, H. J. *Phys. Rev. Lett.* **52**, 1033-1036 (1984).
19. Pietronero, L. & Wiesmann, H. J. *J. statist. Phys.* **36**, 909-916 (1984).
20. Nittemann, J., Daccord, G. & Stanley, H. E. *Nature* **314**, 141-144 (1985).
21. Daccord, G., Nittmann, J. & Stanley, H. E. *Phys. Rev. Lett.* **56**, 336-339 (1986).
22. Chen, J. D. & Wilkinson, D. *Phys. Rev. Lett.* **55**, 1892-1895 (1985).
23. Måløy, K. J., Feder, J. & Jøssang, T. *Phys. Rev. Lett.* **55**, 2688-2691 (1985).
24. Van Damme, H., Obrecht, F., Levitz, P., Gatineau, L. & Laroche, C. *Nature* **320**, 731-733 (1986).
25. Daccord, G. *Phys. Rev. Lett.* **58**, 479-482 (1987).
26. Daccord, G. & Lenormand, R. *Nature* **325**, 41-43 (1987).
27. Meakin, P., Coniglio, A., Stanley, H. E. & Witten, T. A. *Phys. Rev.* A **34**, 3325-3340 (1986).
28. Stanley, H. E. *Introduction to Phase Transitions and Critical Phenomena* (Oxford University Press, 1971).
29. Meakin, P., Stanley, H. E., Coniglio A. & Witten, T. A. *Phys. Rev.* A **32**, 2364-2369 (1985).
30. Halsey, T. C., Meakin, P. & Procaccia, I. *Phys. Rev. Lett.* **56**, 854-857 (1986).
31. Amitrano, C., Coniglio, A. & di Liberto, F. *Phys. Rev. Lett.* **57**, 1016-1019 (1987).
32. Nittmann, J., Stanley, H. E., Touboul, E. & Daccord, G. *Phys. Rev. Lett.* **58**, 619 (1987).
33. Jensen, M. H., Kadanoff, L. P., Libchaber, A., Procaccia, I. & Stavans, J. *Phys. Rev. Lett.* **55**, 2798-2801 (1985).
34. Coniglio, A. in *On Growth and Form: Fractal and Non-Fractal Patterns in Physics* (eds Stanley, H. E. & Ostrowsky, N.) 101 (Nijhoff, Doredrecht, 1985).
35. Halsey, T. C., Jensen, M. H., Kadanoff, L. P., Procaccia, I. & Shraiman, B. *Phys. Rev.* A **33**, 1141-1151 (1986).
36. Coniglio, A. in *Fractals in Physics* (eds Pietronero, L. & Tosatti, E.) (North-Holland, Amsterdam, 1986).
37. Coniglio, A. *Physica* A **140**, 51-61 (1986).
38. Meakin, P. *Phys. Rev.* A **34**, 710-713 (1986).
39. Grassberger, P. & Procaccia, I. *Physica* **13D**, 34-54 (1984).
40. Grassberger, P. *Phys. Lett.* **107A**, 101-105 (1985).
41. Benzi, R., Paladin, G., Parisi, G. & Vulpiani, A. *J. Phys. A* **17**, 3521-3531 (1984); *Ibid.* **18**, 2157-2165 (1985).
42. Badii, R. & Politi, A. *J. statist. Phys.* **40**, 725-750 (1985).
43. Stauffer, D. *Introduction to Percolation Theory* (Taylor and Francis, Philadelphia, 1985).
44. Rammal, R., Tannous, C., Breton, P. & Tremblay, A. M. S. *Phys. Rev. Lett.* **54**, 1718-1721 (1985).
45. de Arcangelis, L., Redner, S. & Coniglio, A. *Phys. Rev.* B **31**, 4725-4727 (1985); *Phys. Rev.* B **34**, 4656-4673 (1986).
46. Rammal, R., Tannous, C. & Tremblay, A. M. S. *Phys. Rev.* A **31**, 2662-2671 (1985).
47. Rammal, R. *J. Phys., Paris* **46**, L129 (1985); *Phys. Rev. Lett.* **55**, 1428 (1985).
48. Meir, Y., Blumenfeld, R., Aharony, A. & Harris, A. B. *Phys. Rev.* B **34**, 3424-3428 (1986).
49. Blumenfeld, R., Meir, Y., Harris, A. B. & Aharony, A. *J. Phys.* A **19**, L791-L796 (1986).
50. Blumenfeld, R., Meir, Y., Aharony, A. & Harris, A. B. *Phys. Rev.* B **35**, 3524-3535 (1987).
51. Meir, Y. & Aharony, A. *Phys. Rev.* A **37**, 596-600 (1988).
52. Rammal, R. & Tremblay, A.-M. S. *Phys. Rev. Lett.* **58**, 415-418 (1987).
53. Fourcade, B., Breton, P. & Tremblay, A.-M. S. *Phys. Rev. Lett.* (in the press).
54. Stanley, H. E. *J. Phys.* A **10**, L211-L220 (1977).
55. Coniglio, A. *Phys. Rev. Lett.* **46**, 250-253 (1981).
56. Coniglio, A. *J. Phys.* A **15**, 3829-2844 (1981).
57. Pike, R. & Stanley, H. E. *J. Phys.* A **14**, L169-L177 (1981).
58. Herrmann, H. J. & Stanley, H. E. *Phys. Rev. Lett.* **53**, 1121-1124 (1984).
59. Alstrøm, P. in *Time-Dependent Effects in Disordered Materials* (eds Pynn, R. & Riste, T.) 185-193 (Plenum, New York, 1987); *Phys. Rev.* A **37**, 1378-1380 (1988); *Phys. Rev.* A **36**, 827-833 (1987).
60. Frisch, U., Sulem, P. & Nelkin, M. *J. Fluid Mech.* **87**, 719-736 (1978).
61. Meakin, P. *Phys. Rev.* A **36**, 2833-2837; *J. Phys.* A **20**, L779-L784 (1987).
62. Lovejoy, S. & Schertzer, D. *Bull. Am. met. Soc.* **67**, 221 (1986).
63. Lovejoy, S., Schertzer, D. & Tsonis, A. A. *Science* **231**, 1036-1038 (1987).
64. Schertzer, D. & Lovejoy, S. in *IUTAM Symposium on Turbulence and Chaotic Phenomena in Fluids, Kyoto, Japan* 141-144 (1983).
65. Mandelbrot, B. B. *J. Fluid Mech.* **62**, 331-358 (1974).
66. Mandelbrot, B. B. in *Proc. 13th IUPAP Conference on Statistical Physics* (eds Cabib, E., Kuper, C. G. & Reiss, I.) (Hilger, Bristol, 1978).
67. Grassberger, P. *Phys. Lett.* A **97**, 277-230 (1983).
68. Hentschel, H. G. E. & Procaccia, I. *Physica* **8D**, 435-444 (1983).
69. Frisch, U. & Parisi, G. in *Turbulence and Predictability in Geophysical Fluid Dynamics and Climate Dynamics* Proc. Int. School of Physics Enrico Fermi, Course LXXXVIII (eds Ghil, M., Benzi, R. & Parisi G.) (North-Holland, Amsterdam, 1985).
70. Katzen, D. & Procaccia, I. *Phys. Rev. Lett.* **58**, 1169-1172 (1987).
71. Cates, M. E. & Witten, T. A. *Phys. Rev. Lett.* **56**, 2497-2500 (1986); *Phys. Rev.* A **35**, 1809-1824 (1987).
72. Evertsz, C. & Lyklema, J. W. *Phys. Rev. Lett.* **58**, 397-400 (1987).
73. Lyklema, J. W., Evertsz, C. & Pietronero, L. *Europhys. Lett.* **2**, 77-82 (1986).
74. Lyklema, J. W. & Evertsz, C. *J. Phys.* A **19**, L895-L900 (1986).
75. Pietronero, L. & Siebesma, A. *Phys. Rev. Lett.* **57**, 1098-1101 (1986).
76. Waissmann, H. & Havlin, S. *Phys. Rev.* B **37**, 5994-5997 (1988).
77. Trus, B., Havlin, S & Stauffer, D. *J. Phys.* A **20**, 6627-6630 (1987).